

Controllable Electrochemical Synthesis and Photovoltaic Performance of Bismuth Oxide/Graphene Oxide Nanostructure Arrays

Fatma Bayrakçeken Nişancı^{1*}

¹ Department of Chemistry, Faculty of Sciences, Atatürk University, Erzurum, Türkiye

Article History

Received: 21.12.2021

Accepted: 18.03.2022

Published: 25.09.2022

Research Article

Abstract – The electrodeposition coated graphene oxide (GO) sheets on semiconductor metal oxide substrates are reduced to produce transparent, flexible, and conductive electrodes. Electrochemically produced bismuth oxide nanoflower films with high crystallinity were characterized by depositing reduced graphene oxide (GO) films on top. The influence of coating period on the shape, structure, and characteristics of electrochemically formed metal oxides was also examined. The graphene oxide modified metal oxide electrode was successfully manufactured using an electrochemical method and characterized using potential controlled electrochemical deposition, atomic force microscopy, scanning electron microscopy, energy dispersive spectroscopy, X-ray diffraction techniques, and Raman measurements. By controlling the deposition period, we can regulate the form and size of electrodeposited bismuth oxide/graphene oxide nanostructures using this electrochemical method from aqueous bismuth oxide/graphene oxide suspensions. The nanostructured bismuth oxide/graphene oxide electrode that results has high photovoltaic characteristics and can be employed in solar energy conversion applications. Our findings suggest that indium tin oxide (ITO) or bismuth oxide-GO films on gold electrodes may be used to enhance surface area in electrochemical synthesis, and that it is conceivable to synthesize semiconductor metal oxides in GO films for future flexible photovoltaic applications.

Keywords – GO, Bi_2O_3 , electrochemical deposition, photovoltaic cell, thin films.

1. Introduction

Nanomaterials including titanium oxide (TiO_2), silicon oxide (SiO_2), silver, iridium oxide, graphene, bismuth (III) oxide (Bi_2O_3), and fullerenes, among others, are commonly employed in electrochemical sensors and biosensors. These biosensors have been effectively employed for sensor preparation, and they are stable and simple to make. Because of its distinctive features such as energy bandgap, wide surface area, electrochemical stability, and excellent catalytic activity applications, Bi_2O_3 is regarded one of the most encouraging electrode substances for electrochemical sensing devices among all nanomaterials. Its sensitivity, electrical conductivity, chemical stability and a favourable electrochemical sensor for voltammetric measurement have all been demonstrated (Anandan et al, 2010). Bismuth(III) oxide is also non-toxic and chemically inert, as well as biocompatible.

Nanoscale bismuth(III) oxide offers more benefits than macroscale bismuth(III) oxide, and its higher surface free energy makes it suited for biomolecule adsorption. The usage areas of GO material are expanding day by day due to its dielectric properties, transparency, ease of solubility in solutions, adjustable electronic properties as well as superior mechanical properties. (McAllister et al., 2007, Anandan et al, 2010, Kim et al, 2012, Mathkar et. al, 2012). It has also turn up as one of the most strong competitors among the most common UV-active TiO_2 photocatalyst, especially Bi_2O_3 (Kamat, 2011). Bismuth is non-poisonous in its oxide shapes and can be used in active apps such as piezoelectric material (Kuma&Devi, 2011), biosensors functional glasses, etc. (Panda, 2009). Current research on the photocatalytic activities of the distinct phases of Bi_2O_3 indicates that they are non-toxic and resistant to photo corrosion (Ünlü et al, 2021, Molinari et al, 2020). In combinations such as Au-loaded α - Bi_2O_3 (Taufik et al, 2011- Eberl& Kisch, 2008).

¹ fbayrakceken@atauni.edu.tr

*Corresponding Author

and Ag-loaded β - Bi_2O_3 (Zhu et al,2011- Jiang et al, 2012), activity is seen to be improved in noble metal nanoparticles. Bi_2O_3 -GO modified electrodes were successfully synthesized on ITO electrochemically. In electrochemically synthesized Bi_2O_3 -GO thin films, GO structures covering Bi_2O_3 nanoflower structures like a transparent sheet will find use in many application areas such as ideal electrochemical performance and superordinate electroactive plane region such as sensors.

2. Materials and Methods

In our electrochemical tests, we employed a BAS 100 B/W electrochemical workstation with three electrodes. For electrochemical studies, we employed an Ag/AgCl electrode as the reference electrode, a platinum wire as the counter, and ITO coated quartz (10 cm^2) as the working electrode in all cases. Dissolved O_2 gas, $1\text{ mM Bi}(\text{NO}_3)_3$, pH 1.5 At room temperature, electrochemical Bi_2O_3 /GO film deposition was executed. For 30 minutes, maintain a steady voltage of $+300\text{ mV}$. The Bi_2O_3 /GO working electrode was dried at room temperature, and the film was cured for roughly one minute with warm air. The GO ($+1000\text{ mV}$) modification was applied electrochemically to ensure that the surfaces generated by the potential controlled electrolysis process of nanostructured Bi_2O_3 films on ITO substrates at a constant voltage ($+300\text{ mV}$) had a high surface area (Figure 1). The morphological and structural examination of synthesized thin films was performed using atomic force microscopy (AFM), scanning electron microscopy (SEM) and x-ray diffraction (XRD), energy dispersive spectroscopy (EDS) for qualitative and quantitative analysis, and photocurrent spectroscopy for photocurrent measurements. A Rigaku powder X-ray diffractometer with a Cu K X-ray source ($\lambda = 1.5406$) was used to record powder X-ray diffractograms of the deposited films. By performing Bi_2O_3 -GO surface characterization with SEM, AFM images, it was possible to examine the surfaces at atomic and molecular dimensions, and Zeiss/Sigma 300 model SEM, Hitachi HT770 brand TEM, and Hitachi S100N brand AFM systems were used respectively for this. Raman spectra were determined by using the WITech alpha 300R device and the bonds made by the atoms or molecules that make up the Bi_2O_3 -GO in their analysis in the range of $1000\text{-}3500\text{ cm}^{-1}$.

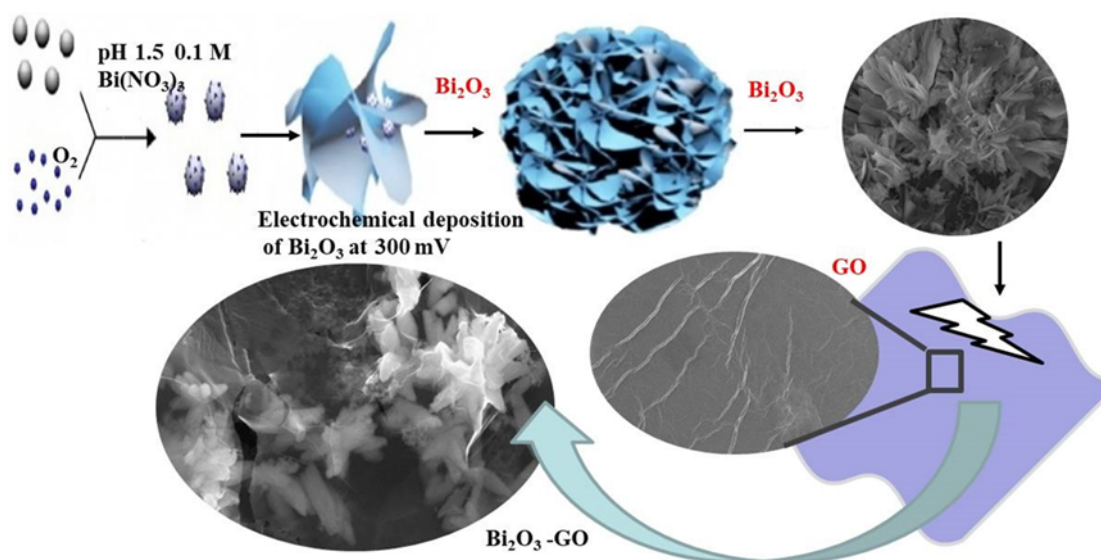


Figure 1. Schematic representation of the electrochemical formation of Bi_2O_3 -GO thin films.

3. Results and Discussion

Figure 2 show the SEM image and EDS spectra taken after electrochemical Bi_2O_3 -GO deposition. Bi_2O_3 -GO nanostructures electrodeposited on ITO electrodes consist of nanoflower and GO film wrapped like a transparent sheet (Figure 2a). This observation shows that the deposition potential and concentration, which provides a significant effect in the morphology-controlled synthesis of Bi_2O_3 nanostructures, remain Bi_2O_3 constant throughout the electrochemical treatment. These results also show that the surface area is increased as much as possible by coating the Bi_2O_3 films with GO films (Cruz-Silva et al. 2016). The EDS spectrum in Figure 2b also indicates that, similar to the XRD spectrum, the Bi_2O_3 -GO nanostructures contain no

impurities other than trace quantities of Cl^- and K^+ induced by reference electrode leakage. XPS analyses were implemented to achieve more detailed split on the type of surface components in Bi_2O_3 -GO films, which were partially analyzed qualitatively by EDS technique, and determine the oxidation steps of these components.

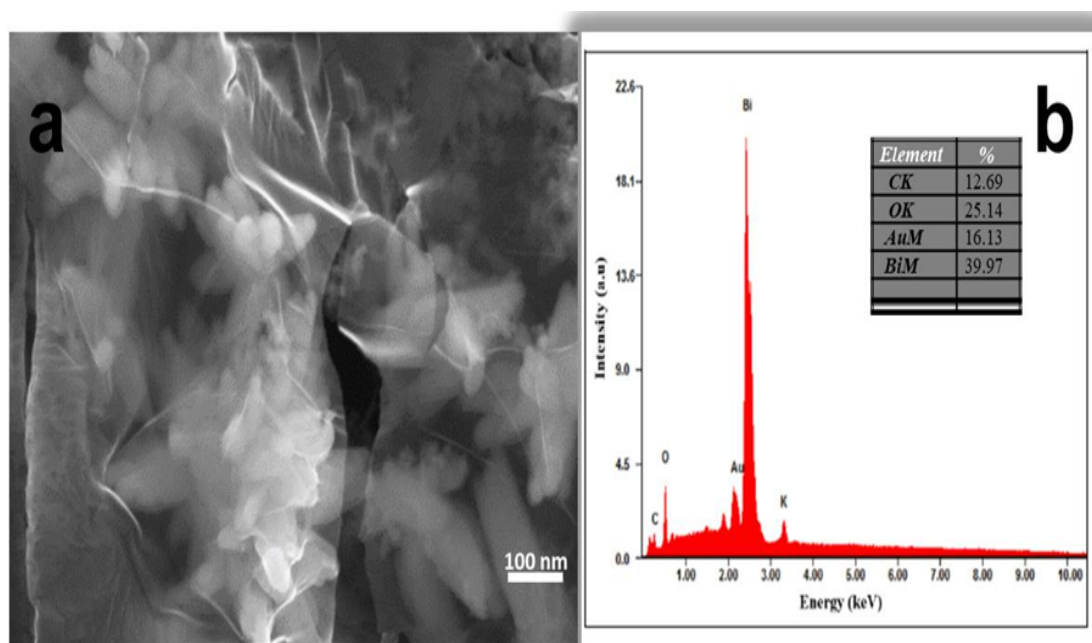


Figure 2. a) SEM image of electrochemically magnified films of Bi_2O_3 -GO on ITO electrode, (b) EDS spectrum of Bi_2O_3 -GO films.

In the XRD diffractogram of the electrodeposited Bi_2O_3 at $2\theta=30,245^\circ$ de, the diffraction peaks of GO at $2\theta=39.838$, Bi_2O_3 -GO at $2\theta=35,468$, and other peaks of the ITO substrate as the working electrode (Figure 3) are clearly seen (Yang&Lin, 2020). The observation of a single and very strong (201) peak belonging to the Bi_2O_3 -GO phase indicates that it has a preferential electrochemical growth orientation.

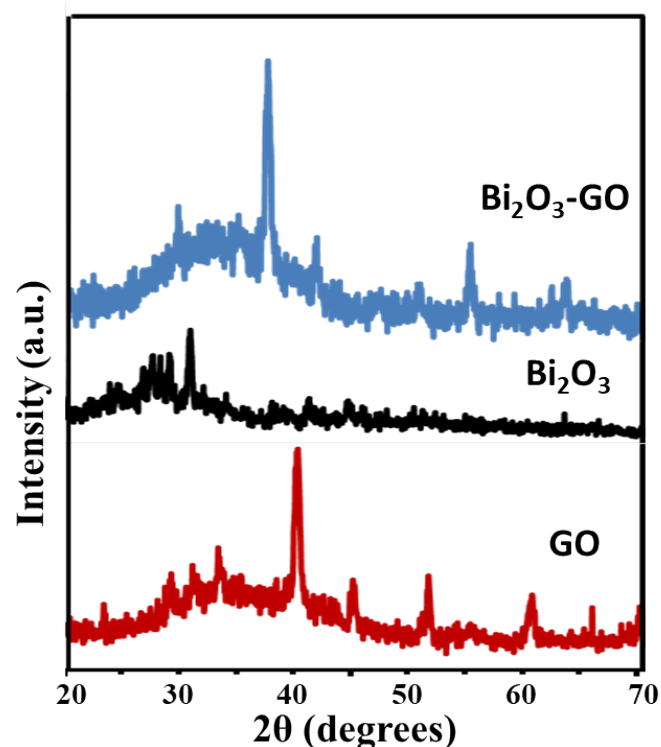


Figure 3. XRD spectrum of GO, Bi_2O_3 , and Bi_2O_3 -GO.

AFM data of GO, Bi_2O_3 , and Bi_2O_3 -GO are given in Figure 4. In the AFM data, as in the 3D images of GO and Bi_2O_3 thin films, GO thin films are homogeneously completely coated on the ITO electrodes, while Bi_2O_3 shows morphological properties like a nanoflower. In the AFM data of Bi_2O_3 -GO, the Bi_2O_3 nanoflower surface is covered with a completely transparent GO film.

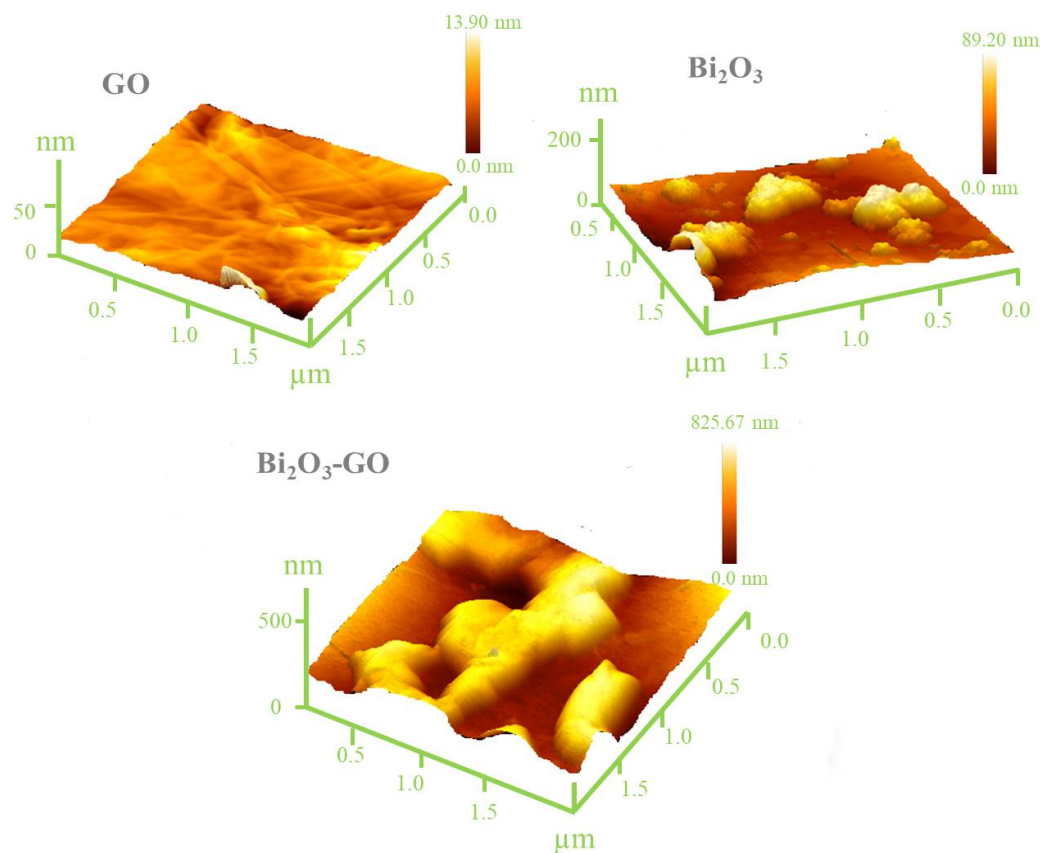


Figure 4. 3D AFM images of GO, Bi_2O_3 , and Bi_2O_3 -GO.

XPS (Figure 5a) analyses were implemented to acquire more detailed diagnose the type of surface components in Bi_2O_3 -GO films and to determine the oxidation steps of the components, which were partially analyzed qualitatively by the Raman technique. The positions of the binding energies of the Bi 4f peaks in the synthesized samples (158.8 eV-164.3 eV for Bi 4f 7/2 and 4f 5/2, seriatim) (Figure 5b) match exactly with the Bi_2O_3 standard data (Oprea et al, 2013). It is clearly seen that the peak in the XPS spectrum obtained for O1s is broad and asymmetrical. The nature of this peak, centered at 530.8 eV, observed for Bi_2O_3 -GO films corresponds to diverse bindings of oxygen in the surfaces. It is formed by the combination of the binding energies of this XPS peak of 529.7 eV, 530.7 eV, and 531.9 eV (Figure 5c). The weak peaks are due to the weakly bonded oxygen and hydroxyl groups to the film surface.

Photoelectrochemical performance of Bi_2O_3 -GO thin films was gauged in a 3 electrode quartz window cell connected to a potentiostat and polar simulator (Figure 6). Photocurrent transitions of Bi_2O_3 -GO structures obtained as a result of illumination at various intervals with artificial sunlight are given in Figure 6. Photocurrents were measured every 8 seconds in the dark and in the light in 0.1 M Na_2SO_4 without any reagents or catalysis. When the Bi_2O_3 -GO electrode is illuminated, a rapid increase is seen in the photocurrent value from 4.9 mA cm^{-2} to 10 mA cm^{-2} . Since the crystal is not ideal, there are entrapment or recombination centers such as defects. When the Bi_2O_3 -GO electrode is illuminated, the photocurrent value increases rapidly and then remains constant, which is explained by the decrease in the trap and recombination centers due to the defects in the electrode structure, thus keeping the carriers in the conduction band less at the defect levels (Sirimanne et al 2002). When the excitation source is turned off, the excess carriers return to the equilibrium value and cause the photocurrent

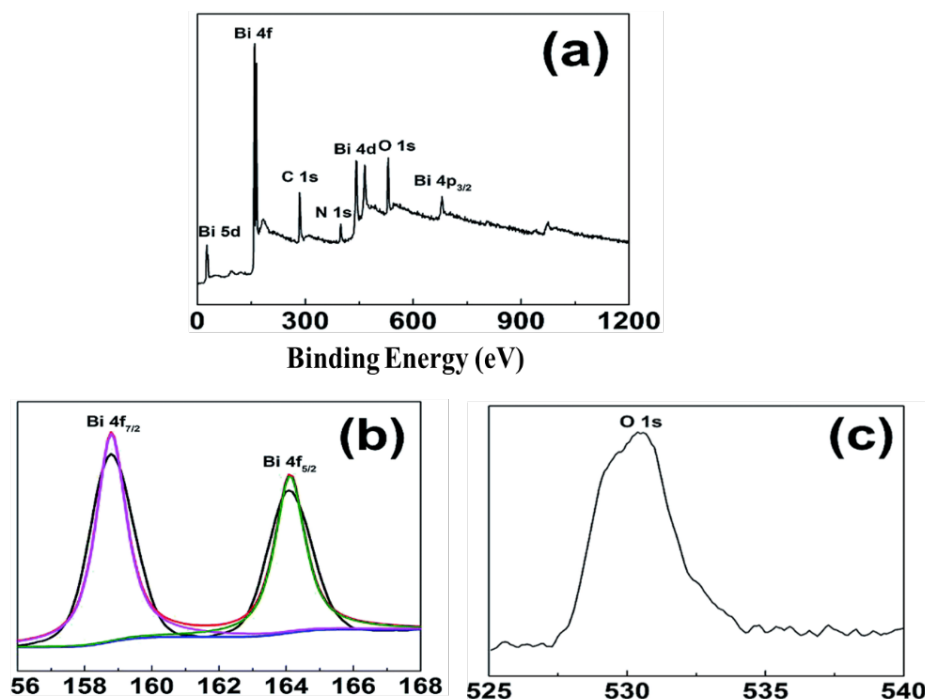


Figure 5. XPS data of Bi_2O_3 -GO (a) full-scan XPS spectrum, (b) Bi 4f spectrum and (c) O 1s spectrum.

value to decrease. These fast and homogeneous photocurrent transitions shown indicate that charge transmission in the material is progressing rapidly. This can repeat over many cycles as stable regardless of electrode photocorrosion.

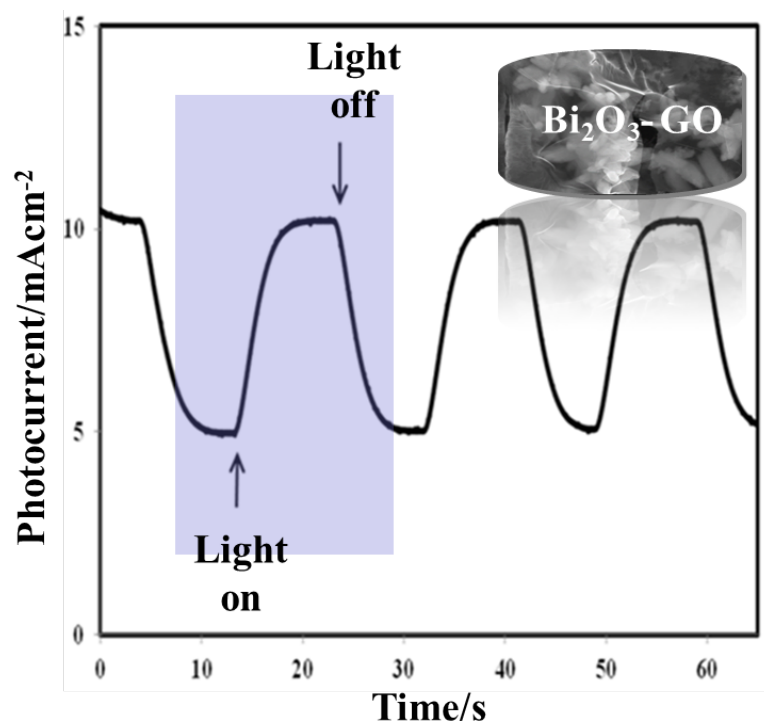


Figure 6. Photocurrent transitions of Bi_2O_3 -GO photoanode under discrete artificial sunlight.

Raman spectra of GO, Bi_2O_3 , Bi_2O_3 -GO structures are given in Figure 7. GO structures have D and G bands available (Qin et al, 2014). Only in Bi_2O_3 films, Bi-O stresses begin in the range of 120-150 cm^{-1} , while coordination vibrations occur in the range of 200-400 cm^{-1} , and weak peaks are caused by oxygen

and hydroxyl groups weakly attached to the film surface. In Bi_2O_3 – GO thin films, the switch of the G band from 1601 cm^{-1} to 1621 cm^{-1} on Bi_2O_3 surfaces coated with GO proves that there is a charge transfer from GO to Bi_2O_3 (Rubbens et al, 2007). Also, this shift from blue to red indicates the existence of an electrical force linking atoms and allogamy between the GO and Bi_2O_3 layers.

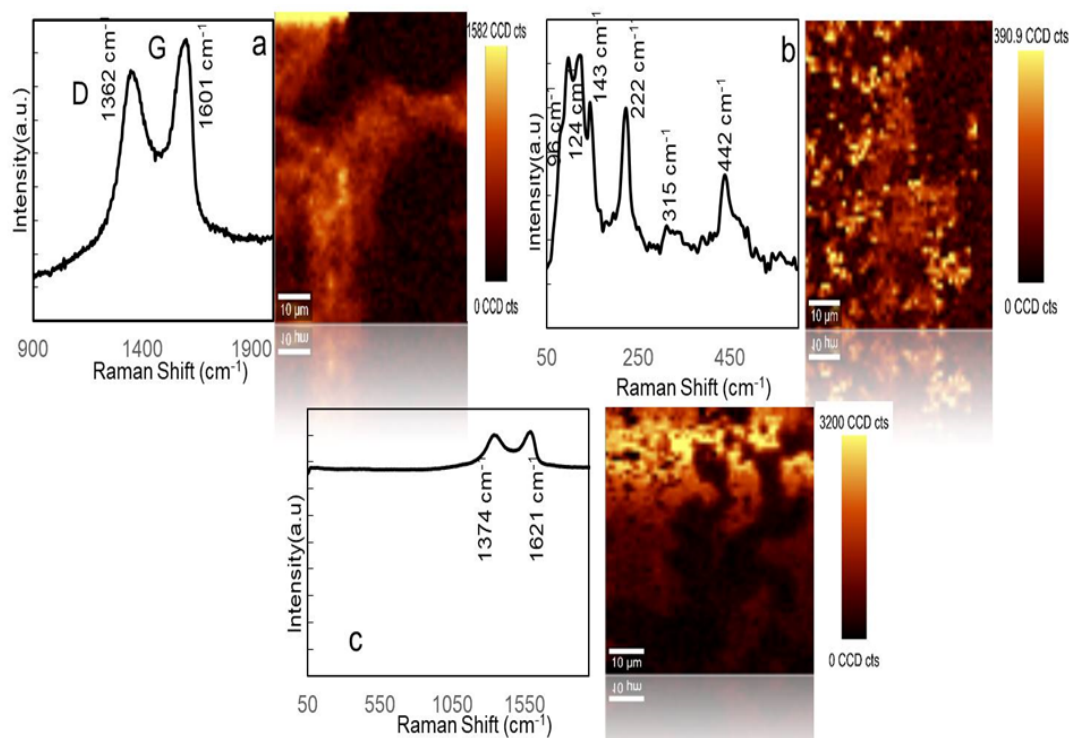


Figure 7. Raman data of (a) GO; (b) Bi_2O_3 ; (c) Bi_2O_3 – GO structures.

4. Conclusion

Bi_2O_3 -GO modified electrodes were successfully synthesized on ITO electrochemically. These heterostructured composites were fully characterized by AFM, SEM, XRD, and Raman spectroscopy and benefited from solar energy applications. The photocurrent transitions of these films also showed homogeneous photocurrent signals, indicating that charge transmission in this material is fast and that the Bi_2O_3 – GO thin films are in a crystalline structure. As a result, metal oxide semiconductor materials have strong photovoltaic characteristics and may be utilized for solar energy conversion and other applications with high performance.

References

- Anandan, S., Lee, G. J., Chen, P. K., Fan, C., & Wu, J. J. (2010). Removal of orange II dye in water by visible light assisted photocatalytic ozonation using Bi_2O_3 and $\text{Au}/\text{Bi}_2\text{O}_3$ nanorods. *Industrial & engineering chemistry research*, 49(20), 9729-9737. DOI: <https://doi.org/10.1021/ie101361c>
- Eberl, J., & Kisch, H. (2008). Visible light photo-oxidations in the presence of $\alpha\text{-Bi}_2\text{O}_3$. *Photochemical & Photobiological Sciences*, 7(11), 1400-1406. DOI: <https://doi.org/10.1039/b811197a>
- Jiang, H. Y., Cheng, K., & Lin, J. (2012). Crystalline metallic Au nanoparticle-loaded $\alpha\text{-Bi}_2\text{O}_3$ microrods for improved photocatalysis. *Physical Chemistry Chemical Physics*, 14(35), 12114-12121. DOI: <https://doi.org/10.1039/C2CP42165H>
- Kamat, P. V. (2011). Graphene-based nanoassemblies for energy conversion. *The Journal of Physical Chemistry Letters*, 2(3), 242-251. DOI: <https://doi.org/10.1021/jz101639v>

- Kim, S., Zhou, S., Hu, Y., Acik, M., Chabal, Y. J., Berger, C., ... & Riedo, E. (2012). Room-temperature metastability of multilayer graphene oxide films. *Nature materials*, 11(6), 544-549. DOI: <https://doi.org/10.1038/nmat3316>
- Kumar, S. G., & Devi, L. G. (2011). Review on modified TiO₂ photocatalysis under UV/visible light: selected results and related mechanisms on interfacial charge carrier transfer dynamics. *The Journal of physical chemistry A*, 115(46), 13211-13241. DOI: <https://doi.org/10.1021/jp204364a>
- Molinari, R., Lavorato, C. and Argurio, P. (2020). Visible-Light Photocatalysts and Their Perspectives for Building Photocatalytic Membrane Reactors for Various Liquid Phase Chemical Conversions. *Catalysts*, 10, 1334. DOI: <https://doi.org/10.3390/catal10111334>
- Mathkar, A., Tozier, D., Cox, P., Ong, P., Galande, C., Balakrishnan, K., ... & Ajayan, P. M. (2012). Controlled, stepwise reduction and band gap manipulation of graphene oxide. *The journal of physical chemistry letters*, 3(8), 986-991. DOI: <https://doi.org/10.1021/jz300096t>
- McAllister, M. J., Li, J. L., Adamson, D. H., Schniepp, H. C., Abdala, A. A., Liu, J., ... & Aksay, I. A. (2007). Single sheet functionalized graphene by oxidation and thermal expansion of graphite. *Chemistry of materials*, 19(18), 4396-4404. DOI: <https://doi.org/10.1021/cm0630800>
- Oprea, O. B., Radu, T., Simon, S. (2013). XPS investigation of atomic environment changes on surface of B₂O₃-Bi₂O₃ glasses. *Journal of Non-Crystalline Solids*, 379(1), 35-39. DOI: <https://doi.org/10.1016/j.jnoncrysol.2013.07.024>
- Panda, P. K. (2009). Environmental friendly lead-free piezoelectric materials. *Journal of materials science*, 44(19), 504. DOI: <https://doi.org/10.1007/s10853-009-3643-0>
- Qin, H., Gong, T., Cho, Y., Leeab, C. and Kim, T. (2014). A conductive copolymer of graphene oxide/poly(1-(3-aminopropyl)pyrrole) and the adsorption of metal ions. *Polymer Chemistry*, 5:4466-4473. DOI: <https://doi.org/10.1039/C4PY00102H>
- Rubbens, A., Drache, M., Roussel, P., & Wignacourt, J. P. (2007). Raman scattering characterization of bismuth based mixed oxides with Bi₂O₃ related structures. *Materials research bulletin*, 42(9), 1683-1690. DOI: <https://doi.org/10.1016/j.materresbull.2006.11.036>
- Cruz-Silva, R., Endo, M. and Terrones, M. (2016). Graphene oxide films, fibers, and membranes. *Nanotechnol Rev*, 5(4), 377-391. DOI: <https://doi.org/10.1515/ntrev-2015-0041>
- Sirimanne, P. M., Takahashi, K., Sonoyama, N., Sakata, T. (2002). Photocurrent enhancement of wide bandgap Bi₂O₃ by Bi₂S₃ over layers. *Solar Energy Materials & Solar Cells* 73, 175-187. DOI: [https://doi.org/10.1016/S0927-0248\(01\)00123-4](https://doi.org/10.1016/S0927-0248(01)00123-4).
- Taufik, S., Yusof, N. A., Tee, T. W., & Ramli, I. (2011). Bismuth oxide nanoparticles/chitosan/modified electrode as biosensor for DNA hybridization. *Int. J. Electrochem. Sci*, 6, 1880-1891.
- Unlü, U., Kemeç, S., Pozan Soylu, G. S. (2021) The impact of alkaline earth oxides on Bi₂O₃ and their catalytic activities in photodegradation of Bisphenol A. *Turkish Journal of Chemistry*, 45: 683-693. DOI: <https://doi.org/10.3906/kim-2101-30>
- Yang, W. D., & Lin, Y. J. (2020). Highly Oriented β -Bi₂O₃-decorated Reduced Graphene Oxide Composites for Supercapacitor Electrodes. *Int. J. Electrochem. Sci*, 15, 1915-1929. DOI: <https://doi.org/10.20964/2020.03.64>
- Zhu, G., Que, W., & Zhang, J. (2011). Synthesis and photocatalytic performance of Ag-loaded β -Bi₂O₃ microspheres under visible light irradiation. *Journal of alloys and compounds*, 509(39), 9479-9486. DOI: <https://doi.org/10.1016/j.jallcom.2011.07.046>